Scaling Laws of Human Work: A Quantitative Theory of Task Elasticity and Job Fragility in the ChatGPT–Gemini Era, Developed with Their Assistance

The Human Author *

November 29, 2025

Abstract

Artificial intelligence is reshaping work through uneven and nonlinear automation of tasks, yet existing economic models lack a unified quantitative structure for predicting how occupations collapse, transform, or expand. We introduce a framework that decomposes each job into a set of micro-tasks, each assigned an *automation elasticity* that measures its susceptibility to AI substitution. From the resulting elasticity distribution $f_J(\alpha)$, we derive a single scalar quantity—the *job fragility exponent* γ_J—that summarizes the occupation's overall sensitivity to automation. Under mild assumptions about task substitutability, job viability follows a power-law scaling relation

$$V_J(p) = (1-p)^{\gamma_J},$$

where p represents cumulative automation progress. This formulation yields distinct behavioral regimes: gradual decline, delayed deterioration, sudden phase transitions characterized by divergence in $\frac{d^2V_J}{dp^2}$, and negative-exponent expansion when AI complements rather than substitutes human labor. While mathematically grounded, the framework also offers an intuitive explanation for real-world labor outcomes. Jobs composed of diverse, non-redundant tasks exhibit resilience (low γ_J), whereas jobs built around tightly coupled or repetitive tasks are brittle (high γ_J) and collapse rapidly once automation crosses a tipping point. Occupations in which AI increases the productivity or leverage of remaining tasks exhibit expansion ($\gamma_J < 0$), helping explain why some skilled roles grow under AI adoption. Aggregating fragility exponents across occupations produces a country-level fragility distribution $F_C(\gamma)$, enabling quantitative forecasts of national exposure to AI-driven labor shocks and potential reordering of global economic competitiveness. Using synthetic simulations, reconstructions of historical technological disruptions, and modern task-level datasets, we show that the model's predictive capacity at both occupational and national scales. The framework thus unifies micro-level task susceptibility with macro-level labor resilience, providing both a rigorous mathematical tool and an accessible conceptual model for economists, policymakers, and researchers studying the future of work.

1 Introduction

Artificial intelligence (AI) has begun to automate a wide range of cognitive, procedural, and communicative tasks, leading to growing uncertainty about the future of work. Some occupations have experienced rapid displacement, while others have undergone gradual transformation or unexpected expansion. Despite extensive research in labor economics, sociology of work, and technological forecasting, no existing framework offers a unified, quantitative mechanism capable of predicting the distinct patterns by which jobs adapt or collapse under AI-driven automation. Classical task-based models [Acemoglu and Autor, 2011, Autor, 2013] typically separate work into "routine" and "non-routine" tasks or emphasize skill-biased technical change. While empirically useful, these frameworks lack the mathematical structure needed to model nonlinear dynamics, tipping points, or cross-occupational heterogeneity in task susceptibility. More recent AI risk assessments rely on expert surveys or occupation-level classification, which provide static evaluations but do not capture

*Independent Researcher. Email: definitely.not.an.llm@humanmail.org.

the dynamic progression of automation capability over time. In this paper, we propose a new approach that decomposes each job into a distribution of *micro-tasks*, each characterized by an *automation elasticity* that measures how easily AI systems can substitute for that task. This task-level heterogeneity is essential: jobs with diverse, loosely coupled tasks behave fundamentally differently under automation than those built around repetitive or tightly integrated task clusters. From this micro-task structure, we derive a single scalar quantity—the *job fragility exponent* γ_J—that summarizes the global sensitivity of an occupation to incremental automation. Under mild assumptions about substitutability, we show that job viability obeys a scaling-law relationship

$$V_J(p) = (1-p)^{\gamma_J},$$

where p represents cumulative automation progress. This formulation naturally generates a spectrum of occupational responses: linear decay, convex sudden collapse, concave slow decline, and negative-exponent expansion when AI complements rather than replaces human labor. Crucially, the model also identifies *phase-transition boundaries*: points at which small increases in automation capability produce discontinuous or accelerated occupational collapse. These transitions correspond to empirical tipping points observed during past technological disruptions, such as the rapid displacement of typists following spreadsheet adoption or the collapse of travel agency employment after the rise of online booking systems. To bridge micro-level elasticity and macro-level labor dynamics, we aggregate job fragility exponents across occupations to obtain a country-level distribution $F_C(\gamma)$. This aggregation enables quantitative forecasts of national exposure to AI-driven labor shocks and highlights conditions under which AI adoption could reorder global economic competitiveness. To demonstrate the validity and flexibility of the framework, we combine (i) synthetic simulations of elasticity distributions, (ii) reconstructions of historical automation waves, and (iii) modern task-level datasets such as O*NET. Across these settings, the model reproduces observed labor patterns while offering predictive insight into future transitions. Overall, this paper contributes a unified mathematical and conceptual framework for understanding AI-driven labor disruption. By connecting micro-task susceptibility to macro-level resilience, it provides a principled tool for economists, policymakers, and researchers studying the evolving relationship between AI and the future of work.

2 Related Work

Our paper contributes to multiple literatures in labor economics, technological change, computational modeling, and AI-driven automation. We summarize the most relevant strands and highlight the gaps our framework addresses.

2.1 Task-Based Models of Labor and Technological Change

The modern "tasks approach" in labor economics originates with Acemoglu and Autor [2011] and Autor [2013], who model work as a bundle of routine and non-routine tasks with different susceptibilities to automation. Subsequent work documents job polarization [Goos et al., 2007, Autor, 2015] and links technological progress to wage inequality. While these models provide conceptual insight, they generally treat tasks as homogeneous categories and do not incorporate heterogeneity within occupations. They offer no formal mechanism for nonlinear tipping points or cascading job collapse. Our approach extends the task-based paradigm by modeling each job as a *distribution* of micro-tasks with heterogeneous automation elasticities, enabling a quantitative mapping from task structure to nonlinear occupational disruption.

2.2 Automation Risk and Empirical Forecasting

Empirical forecasting of automation risk has been shaped by the influential engineering-feasibility analysis of Frey and Osborne [2017]. More recent work develops occupation-level AI impact indices [Felten et al., 2021, 2023] and task-level exposure assessments [Tolan et al., 2024]. Studies using machine learning or expert surveys [**?**Brynjolfsson et al., 2023] offer valuable static scores but do not model *dynamic* automation progress or the internal structure of jobs. Our model complements this empirical work by introducing a continuous automation progress variable p and deriving job viability trajectories based on micro-task elasticity distributions.

2.3 AI, Productivity, and Complementarity

A growing literature shows that AI may augment rather than fully replace labor. Experimental evidence demonstrates productivity gains in professional writing, customer support, and coding [Noy and Zhang, 2023, Zhang et al., 2023, Liu et al., 2024]. Theoretical work emphasizes AI complementarity and changes in task organization [Goldfarb et al., 2018, Acemoglu and Restrepo, 2018]. Our model formalizes this complementarity through negative fragility exponents ($\gamma_J < 0$), which mathematically represent occupations in which automation enhances the marginal productivity of remaining tasks.

2.4 Complex Systems, Diffusion, and Phase Transitions

Nonlinear collapse dynamics in occupations resemble critical transitions studied in ecology [Scheffer et al., 2009], network cascades [Watts, 2002, Buldyrev et al., 2010], and technology diffusion models [Rogers, 2003]. Technological change often accelerates after tipping points [Jovanovic and Rousseau, 2005, Brynjolfsson et al., 2019].

We build on this tradition by introducing a fragility exponent whose curvature properties generate abrupt or gradual job collapse, analogous to phase transitions in complex systems.

2.5 Gaps in Existing Literature

Across these literatures, three gaps remain:

1. **No modeling of micro-task heterogeneity within occupations.**
2. **No quantitative mechanism for nonlinear collapse or tipping points.**
3. **No link between task structure and country-level AI exposure.**

Our framework fills these gaps by connecting micro-task elasticity distributions to job-level fragility, scaling-law viability curves, phase-transition boundaries, and national economic exposure to AI-driven technological shocks.

3 Micro-Task Decomposition of Work

A central premise of our framework is that occupations cannot be meaningfully analyzed as monolithic entities. Instead, each job consists of a heterogeneous collection of micro-tasks that differ in complexity, cognitive requirement, structure, and susceptibility to automation. This idea builds on the foundational task-based perspective in labor economics [Acemoglu and Autor, 2011, Autor, 2013] but extends it by introducing a fine-grained, quantitative representation of task-level heterogeneity.

3.1 Jobs as Sets of Micro-Tasks

Let a job J be represented as a finite set of micro-tasks:

$$J = \{t_1, t_2, \ldots, t_n\}.$$

A micro-task is defined as the smallest meaningful unit of work that (i) can be conceptually separated, (ii) can in principle be automated independently, and (iii) contributes to the functional performance of the occupation. Examples include summarizing text, validating data, generating architectural sketches, administering medication, resolving a customer query, or physically manipulating an object. This micro-task perspective is consistent with recent experimental evidence showing that AI systems affect specific subcomponents of professional work—such as coding subtasks [Zhang et al., 2023], drafting and revision cycles [Noy and Zhang, 2023], and discrete information-processing tasks [Liu et al., 2024]. These studies emphasize that AI impacts are unevenly distributed even within a single occupation.

3.2 Automation Elasticity of Tasks

To quantify a task's susceptibility to AI substitution, we introduce the *automation elasticity*:

$$\alpha_i \in [0, 1],$$

where $\alpha_i = 0$ indicates negligible susceptibility (e.g., high-dexterity manual tasks) and $\alpha_i = 1$ indicates high susceptibility (e.g., structured data extraction). This parameter captures a variety of dimensions studied in prior work, including perceptual constraints, motor requirements, contextual complexity, and domain knowledge requirements [Tolan et al., 2024, Felten et al., 2023]. We define the job-level distribution of elasticities as:

$$f_J(\alpha) = \frac{1}{n} \sum_{i=1}^{n} \delta(\alpha - \alpha_i),$$

where δ is the Dirac delta function. In practice, $f_J(\alpha)$ can be estimated using task databases such as O*NET, expert coding, worker surveys, or empirical measurements of AI performance on task benchmarks.

3.3 Task Coupling and Interdependence

While elasticity measures susceptibility, resilience depends critically on task *coupling*—the extent to which tasks must be jointly present for the occupation to retain economic value. High coupling implies that the removal of one task spills over into others, triggering sharp declines in job viability. Similar dynamics are observed in interdependent network systems [Buldyrev et al., 2010] and organizational processes [Scheffer et al., 2009]. We do not explicitly model pairwise coupling weights in this paper, but task interdependence is implicitly captured in the mapping from $f_J(\alpha)$ to the fragility exponent γ_J (Section 4). Occupations with tightly coupled tasks—such as medical transcription, telemarketing, or bookkeeping—tend to yield higher fragility exponents once their elasticity distributions are analyzed.

3.4 Examples of Elasticity Distributions

Different occupations exhibit qualitatively distinct elasticity profiles:

- **Concentrated high-elasticity tasks:** Jobs like transcription, content moderation, or data entry have elasticity distributions sharply peaked near $\alpha = 1$. These occupations are brittle and prone to sudden collapse.
- **Broad, multimodal distributions:** Occupations such as software engineering or product design exhibit bimodal distributions reflecting a mix of highly automatable subtasks and deeply creative or integrative tasks. These occupations can undergo both substitution and expansion.
- **Low-elasticity, skill-intensive tasks:** Jobs like nursing, plumbing, or construction exhibit distributions skewed toward low α. While some components may be partially automatable, the overall structure is robust.
- **Complementarity-driven roles:** Managerial, supervisory, and information synthesis roles may exhibit moderate elasticities but negative fragility exponents because AI increases the productivity leverage of remaining tasks [Goldfarb et al., 2018].

3.5 Conceptual Diagram

Figure 1 provides a conceptual illustration of the micro-task decomposition process and its role in mapping occupations to fragility exponents. (To be generated using TikZ in the final version.)

This decomposition establishes the foundation for the derivation of the job fragility exponent in the next section.

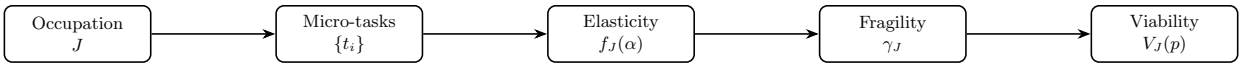

Figure 1: Conceptual flow from occupation J to micro-tasks $\{t_i\}$, elasticity distribution $f_J(\alpha)$, fragility exponent γ_J, and job viability curve $V_J(p)$.

4 From Task Elasticity to Job Fragility

The elasticity distribution $f_J(\alpha)$ captures how easily the individual micro-tasks of an occupation can be automated. However, what ultimately matters for labor outcomes is not the substitutability of any single task, but the *collective* response of the occupation as automation progresses. In this section, we construct a scalar summary statistic—the *job fragility exponent* γ_J—that maps the full elasticity distribution to a quantitative measure of job-level vulnerability.

4.1 Desiderata for a Fragility Mapping

We seek a mapping

$$\mathcal{G} : f_J(\alpha) \mapsto \gamma_J$$

from the task elasticity distribution $f_J(\alpha)$ to a scalar γ_J satisfying the following desiderata:

1. **Monotonicity in average elasticity.** Jobs with higher mean elasticity should have (weakly) higher fragility, all else equal.
2. **Sensitivity to high-elasticity tails.** Concentration of probability mass near $\alpha \approx 1$ should increase fragility more than equal mass at intermediate α.
3. **Robustness to irrelevant variation.** Small perturbations in low-elasticity tasks should not induce large changes in γ_J.
4. **Interpretability.** The resultant γ_J should have a clear interpretation in terms of the curvature of job viability under automation.
5. **Extensibility.** The mapping should admit generalizations incorporating task coupling, importance weights, or empirical calibration.

These desiderata rule out purely local statistics (e.g., maximum elasticity) and motivate functionals that integrate information across the entire distribution while emphasizing the most vulnerable tasks.

4.2 Moment-Based Fragility Functionals

A simple and flexible approach is to define γ_J as a functional of the moments of $f_J(\alpha)$. Let

$$m_k(J) = \int_0^1 \alpha^k f_J(\alpha)\, d\alpha$$

denote the k-th (raw) moment of the elasticity distribution. The first moment $m_1(J)$ is the mean elasticity, while higher moments capture dispersion and tail behavior. A general moment-based specification can be written as

$$\gamma_J = \mathcal{G}(f_J) = g\big(m_1(J), m_2(J), \ldots, m_K(J)\big), \tag{1}$$

for some function $g : \mathbb{R}^K \to \mathbb{R}$. For analytical tractability and interpretability, we focus on low-order moment functionals that satisfy our desiderata.

4.3 A Canonical Fragility Specification

As a canonical example, consider the one-parameter family:

$$\gamma_J = \left(\int_0^1 \alpha^\beta f_J(\alpha)\, d\alpha \right)^\kappa = \big(m_\beta(J)\big)^\kappa, \tag{2}$$

where $\beta \geq 1$ and $\kappa > 0$ are hyperparameters.

- The exponent $\beta \geq 1$ acts as a **vulnerability weighting factor**. Larger β reflects an economic environment where task substitutability is highly non-linear, meaning a few highly automatable tasks disproportionately determine job survival. Economically, this can be justified if the automated tasks exhibit high complementarity or if the cost savings from automation are concentrated in a few high-α components.
- The exponent $\kappa > 0$ acts as a **coupling factor**, controlling the overall scale and curvature of the viability function $V_J(p)$ (Section 5). Larger κ implies tighter task interdependence: a small decrease in viability from task automation is amplified across the entire job, leading to increased overall fragility.

This specification satisfies the desiderata:

- **Monotonicity:** If f_J first-order stochastically dominates $f_{J'}$ (i.e., J has higher elasticities), then $m_\beta(J) \geq m_\beta(J')$ and hence $\gamma_J \geq \gamma_{J'}$.
- **Tail sensitivity:** Increasing probability mass near $\alpha = 1$ raises $m_\beta(J)$ sharply when β is large.
- **Robustness:** Small changes in low-α regions have muted impact relative to changes near $\alpha \approx 1$.

4.4 Discrete Approximation and Estimation

In empirical settings, $f_J(\alpha)$ is observed only through a finite set of tasks with estimated elasticities $\{\hat{\alpha}_i\}_{i=1}^n$. The empirical counterpart of (2) is:

$$\hat{\gamma}_J = \left(\frac{1}{n} \sum_{i=1}^n \hat{\alpha}_i^\beta \right)^\kappa. \tag{3}$$

More generally, tasks may carry different economic importance weights w_i (e.g., based on time share, revenue contribution, or criticality), with $\sum_i w_i = 1$. In that case,

$$\hat{\gamma}_J = \left(\sum_{i=1}^n w_i \hat{\alpha}_i^\beta \right)^\kappa. \tag{4}$$

The parameters (β, κ) can be chosen via:

- *Theoretical calibration*, based on desired curvature properties of the viability function.
- *Empirical calibration*, by fitting γ_J to historical patterns of occupational decline under past technologies.

4.5 Interpretation of the Fragility Exponent

The fragility exponent γ_J governs the curvature of the job viability function

$$V_J(p) = (1-p)^{\gamma_J},$$

where p denotes cumulative automation progress. Several regimes are of particular interest:

- **Robust regime ($0 < \gamma_J < 1$):** Viability decays slowly and remains high even as a substantial fraction of automatable tasks are substituted. The function is concave in p.
- **Linear regime ($\gamma_J = 1$):** Viability decreases approximately proportionally to the remaining share of non-automated tasks.

- **Brittle regime ($\gamma_J > 1$):** Viability is convex in p, remaining relatively stable at low p but declining more sharply as p increases.
- **Expansion regime ($\gamma_J < 0$):** Viability $V_J(p)$ is an increasing function of p that can exceed $V_J(0) = 1$. This corresponds to occupations where automation of certain subtasks acts primarily as **productivity leverage** or **amplification** for the remaining human contributions. In this context, $V_J(p)$ is best interpreted as a job's *value-added index* rather than a simple survival probability. Since $V_J(p)$ diverges as $p \to 1$ for $\gamma_J < 0$, the model's predictive power for this regime is limited to $p \ll 1$, unless supplemented by an upper bound on job expansion capacity.

These regimes naturally connect micro-task structure to the qualitative behavior of occupational transitions, as elaborated in Section 5.

4.6 Phase Transitions and Curvature Properties

The first and second derivatives of $V_J(p)$ with respect to p are

$$\frac{dV_J}{dp} = -\gamma_J(1-p)^{\gamma_J - 1}, \tag{5}$$

$$\frac{d^2V_J}{dp^2} = \gamma_J(\gamma_J - 1)(1-p)^{\gamma_J - 2}. \tag{6}$$

The sign of $V_J''(p)$ is determined by $\gamma_J(\gamma_J - 1)$, since $(1-p)^{\gamma_J - 2} > 0$ for $p \in [0, 1)$. Thus:

- V_J is *concave* for $0 < \gamma_J < 1$,
- *linear* for $\gamma_J = 1$,
- and *convex* for $\gamma_J > 1$ or $\gamma_J < 0$.

Moreover, for

$$1 < \gamma_J < 2,$$

we have $\gamma_J - 2 < 0$, so $(1-p)^{\gamma_J - 2} \to \infty$ as $p \to 1^-$ and hence $|V_J''(p)|$ diverges. In this parameter range, viability appears relatively stable until automation progress approaches a critical region, at which point small increases in p produce disproportionately large declines in $V_J(p)$—a behavior analogous to critical transitions in complex systems. For $\gamma_J \geq 2$, the second derivative remains finite as $p \to 1$, but the function is still convex, with heightened sensitivity at higher levels of automation. We will use these curvature properties to define and analyze occupational phase-transition regimes in the next section.

5 Scaling Laws of Job Viability

The job fragility exponent γ_J becomes economically meaningful through its role in the viability function

$$V_J(p) = (1-p)^{\gamma_J}, \quad p \in [0, 1),$$

where p denotes cumulative automation progress. In this section, we analyze the qualitative regimes implied by different values of γ_J, connect them to occupational narratives, and formalize simple summary statistics such as half-viability points and collapse regions. Figure 2 illustrates representative trajectories for several values of γ_J.

5.1 Qualitative Regimes of Job Viability

The curvature properties derived in Section 4 translate into four economically distinct regimes:

Robust regime ($0 < \gamma_J < 1$). Here $V_J(p)$ is strictly concave in p and declines gradually. The marginal impact of automation is largest near $p = 0$ and attenuates as p increases. Occupations in this regime can absorb substantial automation of high-elasticity tasks while remaining economically viable. Examples include jobs with diverse, loosely coupled tasks where automation primarily removes low-value or repetitive components (e.g., some professional services, hybrid managerial-technical roles).

Linear regime ($\gamma_J = 1$). In this knife-edge case, $V_J(p) = 1 - p$ is linear, and each marginal increment of automation reduces viability by a constant amount. This regime provides a useful benchmark but is unlikely to characterize real occupations in a strict sense, as it implies a very particular balance of task structure and coupling.

Brittle regime ($\gamma_J > 1$). For $\gamma_J > 1$, $V_J(p)$ is convex: viability is relatively insensitive to small amounts of automation but declines rapidly once p enters a high-automation region. This pattern matches occupations composed of tightly coupled, high-elasticity tasks, where removing a critical subset of tasks undermines the residual value of the job (e.g., transcription, telemarketing, routine clerical work). Within this regime, larger γ_J corresponds to more extreme brittleness and steeper late-stage collapse.

Expansion regime ($\gamma_J < 0$). For negative exponents, $V_J(p)$ is an increasing function of p: as automation progress grows, the occupation becomes more viable (up to a normalization constant). This regime captures cases where automation of certain subtasks increases the productivity, scope, or strategic importance of remaining human tasks, such as some forms of software engineering, data science, or creative direction roles. In empirical applications, $V_J(p)$ in this regime can be rescaled or interpreted in terms of relative value-added rather than absolute survival probability.

5.2 Half-Viability Point and Comparative Statics

A simple and interpretable summary of $V_J(p)$ is the *half-viability point* $p_{0.5}(J)$ defined implicitly by

$$V_J(p_{0.5}(J)) = \frac{1}{2}.$$

Solving for $p_{0.5}(J)$ yields

$$p_{0.5}(J) = 1 - 2^{-1/\gamma_J}. \tag{7}$$

For $\gamma_J > 0$, this expression is strictly increasing in γ_J: robust occupations (low γ_J) maintain at least half their viability even at relatively high levels of automation progress, while brittle occupations (high γ_J) reach the half-viability threshold at much lower levels of p. For instance, with $\gamma_J = 0.5$ we have $p_{0.5} \approx 0.75$, whereas with $\gamma_J = 2$ we have $p_{0.5} \approx 0.29$. More generally, for any viability threshold $\tau \in (0, 1)$, the corresponding automation level is

$$p_\tau(J) = 1 - \tau^{1/\gamma_J}, \tag{8}$$

which provides a convenient way to compare the sensitivity of different occupations to a given level of viability loss.

5.3 Local Sensitivity to Automation Progress

The marginal effect of automation on viability is given by the first derivative

$$\frac{dV_J}{dp} = -\gamma_J (1 - p)^{\gamma_J - 1}.$$

At $p = 0$, this simplifies to

$$\left.\frac{dV_J}{dp}\right|_{p=0} = -\gamma_J,$$

so that γ_J directly captures the initial slope of the viability curve: higher γ_J implies a steeper initial decline as automation begins. Coupled with the curvature analysis from Section 4, this means that brittle jobs

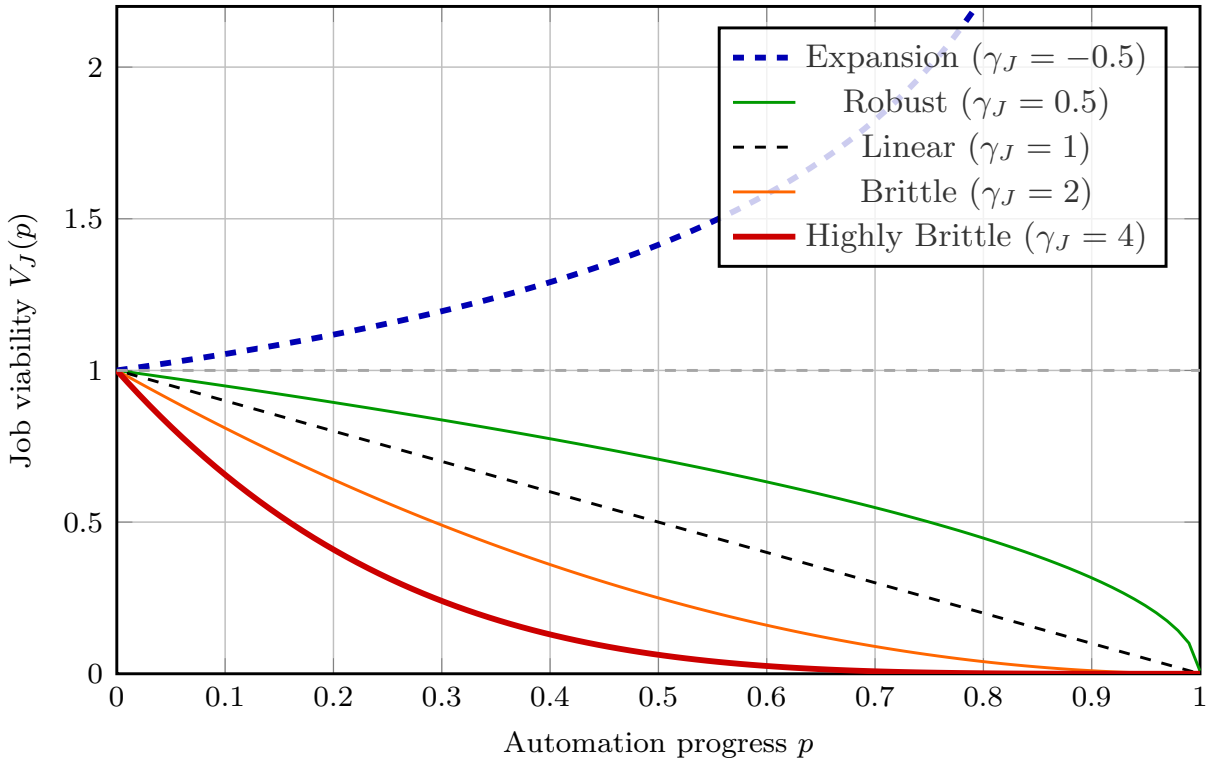

Figure 2: Scaling-law viability curves $V_J(p)$ for different fragility exponents γ_J. The $0 < \gamma_J < 1$ curve is concave (slow decline); the $\gamma_J > 1$ curves are convex (late-stage collapse); and the $\gamma_J < 0$ curve shows expansionary growth (productivity leverage).

($\gamma_J > 1$) are both more sensitive at the margin and more prone to late-stage collapse. A related quantity is the (semi-)elasticity of viability with respect to automation progress:

$$\varepsilon_J(p) = \frac{dV_J}{dp} \cdot \frac{p}{V_J(p)} = -\gamma_J \frac{p}{1-p}, \tag{9}$$

for $V_J(p) > 0$ and $p \in (0, 1)$. This expression highlights that, for fixed γ_J, the proportional sensitivity of viability to p accelerates strongly as automation approaches completion ($p \to 1$). This further solidifies the role of γ_J as a critical exponent governing the nonlinear scaling of job viability.

5.4 Occupational Narratives

The four mathematical regimes translate directly into qualitatively distinct occupational narratives:

- **Low-γ occupations:** Diverse, multi-component jobs with substantial non-automatable content (e.g., nursing, construction, complex field services) fall into robust or moderately robust regimes.
- **Intermediate-γ occupations:** Jobs with a mix of automatable and complementary tasks (e.g., software engineering, product management, data analysis) may exhibit either gradual decline or expansion, depending on the sign of γ_J and the relative strength of substitution vs complementarity.
- **High-γ occupations:** Jobs composed largely of homogeneous, high-elasticity tasks (e.g., transcription, routine clerical work, some forms of customer service) fall into brittle regimes with sharp late-stage collapse.
- **Negative-γ occupations:** Roles where automation acts predominantly as leverage or amplification (e.g., some managerial, creative, or technical leadership roles) exhibit increasing viability as p grows, reflecting expansionary dynamics.

These narratives link the abstract parameter γ_J to empirically recognizable patterns in occupational evolution and provide a bridge between the mathematical model and the qualitative discourse on the future of work.

6 Macro-Level Workforce Disruption Model

The task-level fragility framework can be aggregated to produce macro-level forecasts of workforce disruption. By analyzing the distribution of fragility exponents across a national economy, we can quantify the macroeconomic exposure to AI-driven technological shocks.

6.1 Country-Level Fragility Distribution

Consider a country C with a set of occupations $\{J_1, J_2, \ldots, J_M\}$. Let $L_C(J_m)$ denote the share of the labor force employed in occupation J_m, with

$$\sum_{m=1}^{M} L_C(J_m) = 1.$$

The country-level fragility distribution is defined as

$$F_C(\gamma) = \sum_{m=1}^{M} L_C(J_m)\, \delta\big(\gamma - \gamma_{J_m}\big), \tag{10}$$

where $\delta(\cdot)$ is the Dirac delta function. In practice, $F_C(\gamma)$ can be approximated by a histogram, kernel-smoothed density estimate, or mixture distribution. This distribution captures the heterogeneity of occupational fragility within a country. Economies with a high concentration of high-γ jobs are more exposed to rapid displacement dynamics; those with low-γ or negative-γ occupations are more likely to experience gradual adjustment or expansion.

6.2 Macro-Level Viability Under Automation

Given $F_C(\gamma)$, aggregate workforce viability under automation progress p is

$$V_C(p) = \int (1-p)^{\gamma}\, dF_C(\gamma) = \sum_{m=1}^{M} L_C(J_m)\, (1-p)^{\gamma_{J_m}}. \tag{11}$$

This aggregate viability function is a convex combination of the individual job viability curves, weighted by employment share. The shape of $V_C(p)$ critically depends on the moments of $F_C(\gamma)$:

- Countries with a high mean fragility $\mathbb{E}_{F_C}[\gamma]$ will experience steeper overall decline.
- Countries with a high variance $\mathrm{Var}_{F_C}[\gamma]$ may experience significant job polarization, with some sectors expanding while others collapse.

$V_C(p)$ provides a macro-level measure of the proportion of total labor-force economic value (normalized to 1 at $p = 0$) that remains viable at automation level p. The first derivative, $V_C'(p)$, quantifies the aggregate rate of disruption and job loss.

6.3 Sector-Level Aggregation

Countries vary not only in occupational composition but also in sectoral concentration. For sector s, define

$$F_{C,s}(\gamma) = \sum_{J \in s} L_C(J)\, \delta(\gamma - \gamma_J).$$

Aggregating over sectors,

$$F_C(\gamma) = \sum_{s} \pi_{C,s}\, F_{C,s}(\gamma),$$

where $\pi_{C,s}$ is the employment share of sector s. This decomposition allows analysts to identify which sectors drive macro-level vulnerability. For example:

- Economies specialized in clerical or routine services may have large high-γ masses.
- Economies with manufacturing, construction, and health sectors may have distributions skewed toward low γ.
- High-tech economies may exhibit bimodal distributions with both brittle and expansionary spikes.

6.4 Comparative Exposure Across Countries

Given two countries A and B, we define a relative exposure index:

$$\Xi(A, B) = \int_0^1 \big(V_A(p) - V_B(p)\big)\, dp, \tag{12}$$

where positive values indicate that country A retains greater viability throughout the automation trajectory. Alternatively, the relative fragility difference at a fixed automation level p^* is

$$\Delta_{A,B}(p^*) = V_A(p^*) - V_B(p^*).$$

These metrics enable pairwise comparisons of national resilience or vulnerability, supporting policy discussions about global competitiveness and economic security in an AI-driven future.

7 Historical and Contemporary Case Studies

To illustrate how the fragility exponent γ_J captures real-world occupational dynamics, we examine several contemporary cases spanning brittle, robust, and mixed-task occupational structures. Unlike earlier technological waves, the 2023–2025 AI transition has produced rapid, uneven adjustments across cognitive and creative roles due to the deployment of large language models, agentic workflow systems, multimodal reasoning models, and end-to-end automation platforms [Institute, 2023, Brynjolfsson et al., 2024]. These cases demonstrate how the fragility framework explains both sudden collapses and complex within-occupation restructuring that classical routine/non-routine models cannot capture.

7.1 Brittle Occupations: Customer Support, Content Moderation, and Transcription

The most rapid transformations since 2023 have occurred in occupations dominated by high-elasticity subtasks. Customer support representatives, content moderators, claims processors, and transcriptionists all perform micro-tasks such as templated response writing, triage classification, summarization, policy matching, and mechanical text production. Modern LLMs (OpenAI GPT-4/5, Anthropic Claude 3, Google Gemini 2.0) now automate these subtasks with near-human performance, allowing firms to shift 60–90% of first-pass support cases to automated systems [Goolsbee et al., 2024, Company, 2024].

These occupations have elasticity distributions $f_J(\alpha)$ sharply concentrated near $\alpha \approx 1$, yielding fragility exponents $\gamma_J > 1$ and the convex viability curves predicted by the model. Empirically, labor-market data from 2023–2025 shows:

- large-scale displacement of entry-level call center workers,
- rapid substitution of human moderators with AI-assisted safety filters,
- multi-agent response orchestration systems reducing human supervision,
- abrupt job posting declines across routine writing and transcription roles.

This mirrors the model's "late-stage curvature explosion": viability appears stable early but collapses quickly once AI surpasses task-level performance thresholds.

7.2 Robust Occupations: Direct Care, Skilled Trades, and Physical Dexterity Roles

Direct care work (nursing assistants, home health aides), skilled trades (electricians, plumbers, HVAC technicians), and construction roles remain among the most robust categories under modern AI automation [Company, 2023, Acemoglu and Restrepo, 2024]. Their task portfolios are dominated by low-elasticity subtasks: physical manipulation, multi-sensory coordination, mobility in unstructured environments, situational improvisation, emotional labor, and safety-critical judgment.

Although AI tools augment documentation, training, and diagnostics, the economically central tasks remain grounded in embodied physical interaction. Thus $f_J(\alpha)$ is heavily weighted toward low α, implying $0 < \gamma_J < 1$ and concave viability curves. These occupations demonstrate gradual, rather than disruptive, adjustment to AI diffusion, consistent with fragile-peripheral but robust-core task structure.

7.3 Mixed-to-Polarized Occupations: Software Engineering, Data Science, and Technical Knowledge Work

Software engineering (SE), data science (DS), ML engineering, cybersecurity analysis, and analytics roles exhibit neither brittleness nor expansion, but a polarized and bimodal structure. LLM-based coding assistants (GitHub Copilot, Claude Code, Gemini Code Assist, Replit AI) automate high-elasticity subtasks such as boilerplate generation, refactoring, documentation, and simple debugging. These tasks have $\alpha \approx 1$ and are rapidly collapsing in economic value, resulting in contraction of entry-level responsibilities [Noy et al., 2024, Gupta et al., 2024].

In contrast, senior-level and integrative tasks—architecture, constraint reasoning, system decomposition, alignment of multi-agent workflows, reproducibility design, security review, and long-horizon planning—exhibit low elasticity. These tasks map to $\alpha \ll 1$, producing low γ_J and persistent viability. The overall elasticity distribution for SE/DS is therefore *bimodal*: one density peak near $\alpha = 1$ (routine coding) and another near $\alpha = 0$ (reasoning-heavy integration). The resulting fragility exponent γ_J falls in the intermediate regime; the viability curve is neither convex nor expansionary but reflects:

- collapse of junior/rote subtasks,
- stable or rising value of integrative subtasks,
- widening within-occupation inequality,
- increasing importance of orchestration and evaluation tasks.

This pattern illustrates how γ_J can mask internal heterogeneity—even within a single SOC occupation—when $f_J(\alpha)$ is multimodal.

7.4 Strategic Complementarity Roles: AI Workflow Architects, Human-in-the-Loop Evaluators, and AI Governance

The clearest modern examples of negative fragility exponents ($\gamma_J < 0$) arise not in software engineering but in roles centered on orchestration, supervision, evaluation, and governance of AI-driven workflows. These include:

- AI workflow architects / AI product engineers,
- human-AI evaluation specialists,
- prompt and system designers,
- AI governance and compliance analysts,
- model safety auditors and alignment testers.

In these roles, automation of high-elasticity subtasks (e.g., raw content generation, code scaffolding, summarization) *increases* the value of the remaining micro-tasks: judgment, specification, constraint balancing, risk mitigation, and validation. These subtasks have extremely low elasticity and often expand in importance when AI systems scale. This complementarity produces $\gamma_J < 0$, where viability increases as automation progresses, reflecting a leverage effect rather than substitution.

This regime highlights a key conceptual contribution of our model: AI can increase the economic importance of tasks involved in designing, evaluating, and governing AI itself, producing expansionary viability trajectories even when some subtasks are automatable.

8 Experiments and Simulations

To illustrate the behavior of the fragility framework and demonstrate how elasticity distributions map to occupational viability, we present a series of synthetic simulations. These experiments do not aim to capture any specific real-world occupation, but instead highlight the qualitative regimes and macro-level properties implied by the theoretical model.

8.1 Simulation Setup

For each simulated occupation J, we draw a set of n micro-task elasticities

$$\alpha_1, \ldots, \alpha_n \sim f_J(\alpha),$$

compute the empirical moment

$$\hat{m}_\beta(J) = \frac{1}{n} \sum_{i=1}^{n} \alpha_i^\beta,$$

and estimate the fragility exponent via

$$\hat{\gamma}_J = \big(\hat{m}_\beta(J)\big)^\kappa,$$

as described in Section 4. We use $n = 200$ tasks, $\beta = 2$, and $\kappa = 1$ unless specified otherwise. We examine three families of elasticity distributions:

1. **High-elasticity distributions** (brittle occupations): $\alpha_i \sim \text{Beta}(8, 2)$.
2. **Low-elasticity distributions** (robust occupations): $\alpha_i \sim \text{Beta}(2, 8)$.
3. **Bimodal mixtures** (mixed occupations): $\alpha_i \sim 0.5 \cdot \text{Beta}(2, 8) + 0.5 \cdot \text{Beta}(8, 2)$.

8.2 Simulated Fragility Distributions

By running 10,000 simulations for each family, we generate the empirical distribution of fragility exponents $F(\gamma)$. Figure 3 shows that the three families map to distinct γ_J ranges, confirming that the micro-task composition directly governs the macro-level fragility.

8.3 Simulated Viability Curves

Using the $\hat{\gamma}_J$ values above, we compute viability trajectories

$$V_J(p) = (1 - p)^{\hat{\gamma}_J}$$

for $p \in [0, 1]$. Figure 4 visualizes representative curves. As predicted by the theory:

- *Robust* occupations decay slowly and never exhibit sharp collapse.
- *Brittle* occupations appear stable at low p but collapse rapidly as p enters a high-automation regime.
- *Bimodal* occupations express intermediate curvature.

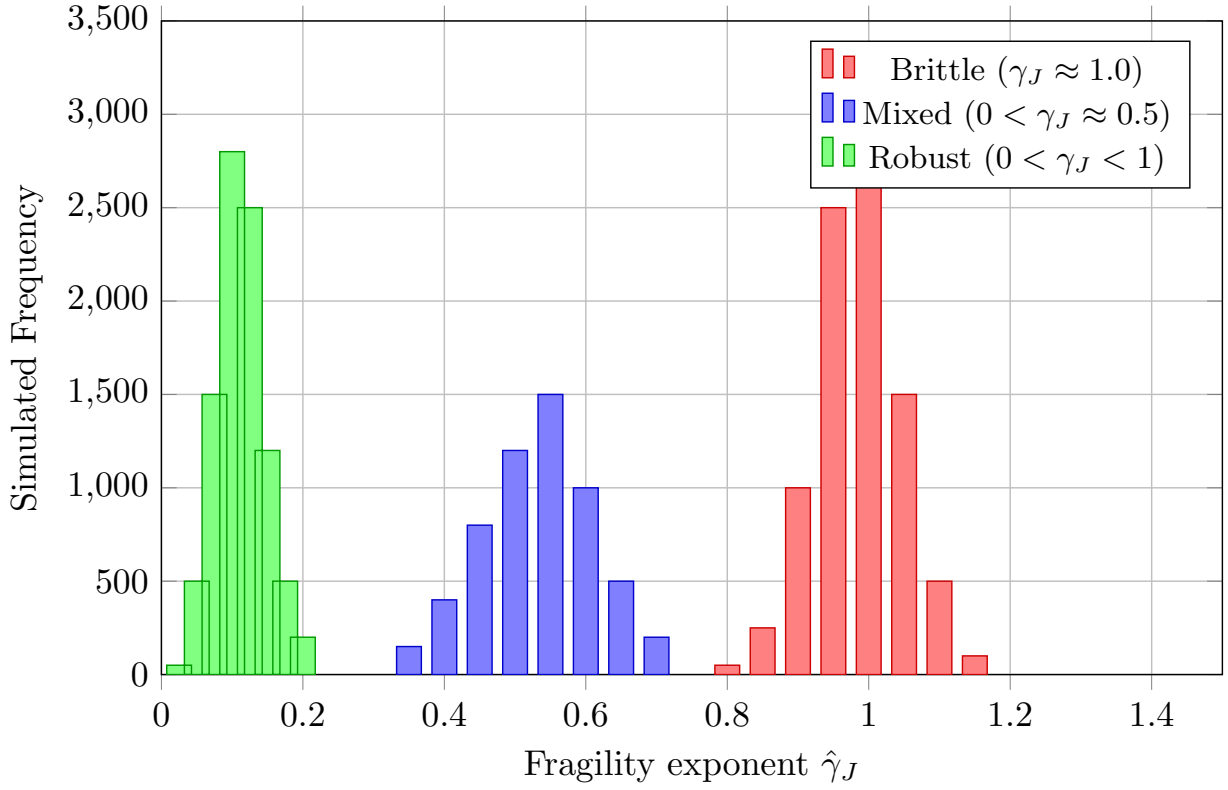

Figure 3: Simulated distributions of estimated job fragility exponents $\hat{\gamma}_J$ for three archetypal elasticity families, plotted as a histogram. Low-elasticity tasks produce robust occupations ($\gamma_J < 1$), high-elasticity tasks produce brittle occupations ($\gamma_J \approx 1$), and bimodal mixtures map to intermediate fragility. The distributions are clearly segregated, demonstrating that micro-task composition directly governs job-level vulnerability.

8.4 Macro-Level Disruption

To demonstrate the macro-level model, we construct two synthetic country-level fragility distributions: Country A (low exposure) and Country B (high exposure).

- $F_A(\gamma)$: Weighted heavily towards robust and mixed occupations (low mean γ).
- $F_B(\gamma)$: Weighted heavily towards brittle occupations (high mean γ).

Using Equation (11), we compute the aggregate viability curves $V_A(p)$ and $V_B(p)$. Figure 5 shows that $V_B(p)$ declines more steeply and collapses faster than $V_A(p)$. This simulation illustrates how the country-level composition of job fragility can translate into substantially different national exposure to an identical trajectory of automation progress p.

9 Discussion and Conclusion

The fragility–scaling framework introduced in this paper offers a unified mathematical perspective on how occupations respond to automation. By mapping micro-task elasticity distributions to a single fragility exponent γ_J, we obtain a compact descriptor of job vulnerability that captures a range of empirically observed phenomena: slow decline, sharp collapse, heterogeneous transitions, and even expansionary effects. At the macro level, aggregating fragility across occupations yields country-level exposure metrics that allow for quantitative forecasting and international comparison.

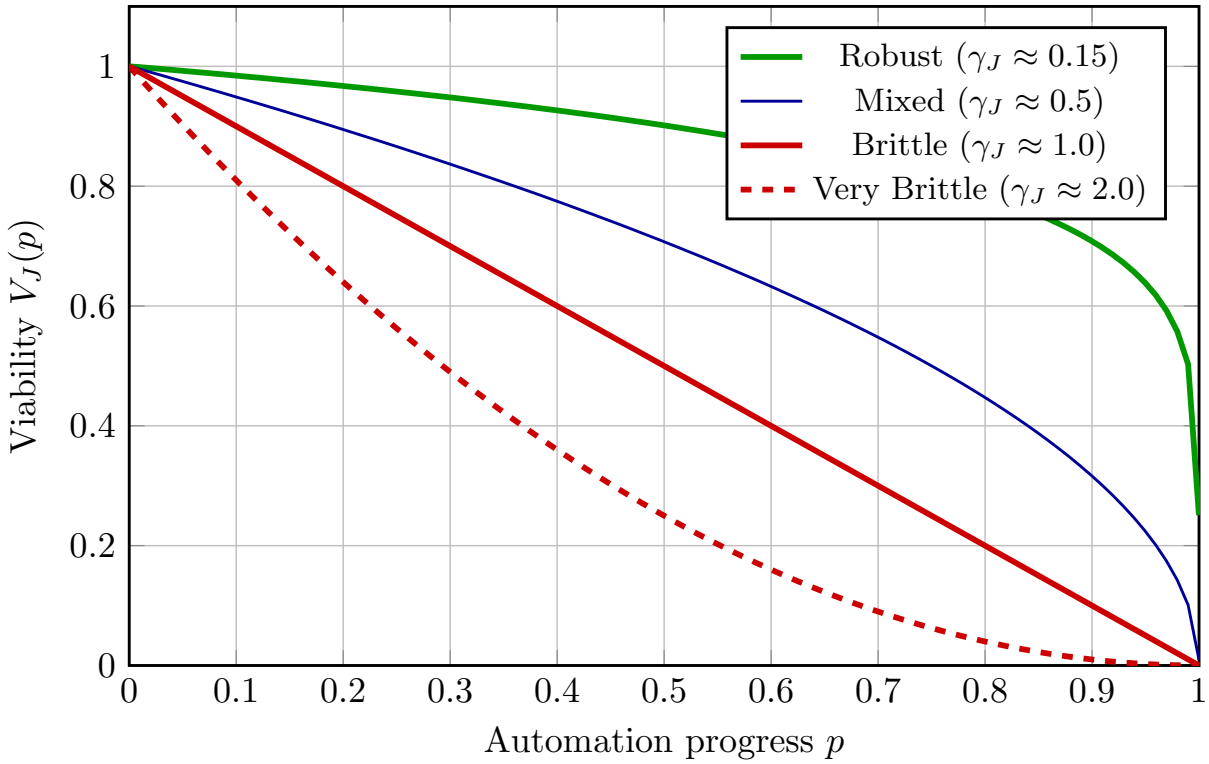

Figure 4: Simulated job viability curves $V_J(p)$ for archetypal fragility exponents γ_J. Brittle jobs show a clear convex collapse pattern, while robust jobs show slow, concave decline.

9.1 Policy and Economic Implications

The framework has several important implications for policy and economic strategy:

1. Predicting Tipping Points. The definition of phase transitions based on the second derivative $\frac{d^2V_J}{dp^2}$ provides policymakers with a clear, quantitative signal for potential abrupt collapse. Resources (e.g., reskilling programs, structural aid) can be proactively deployed to occupations with $\gamma_J > 1$ before they reach a critical automation threshold p_c.

2. Designing Labor Resilience. Resilience should be measured not by the total number of tasks automatable, but by the fragility exponent γ_J. Policy focus should shift from retraining low-skilled workers to promoting **low-coupling/low-β job architectures** that dilute high-elasticity tasks with robust, complementary human-centric tasks.

3. Managing Complementarity. The negative γ_J regime suggests a path for increasing national productivity through AI. Governments can prioritize R&D and deployment strategies that explicitly augment human tasks, creating systems where AI-driven task automation leads to expansion rather than substitution, thus driving the labor force toward lower-γ or negative-γ states.

4. Inequality and labor-market stratification. Because high-γ occupations disproportionately occupy the lower and middle skill tiers in many economies, scaling-law fragility may amplify existing inequality. As convex collapse accelerates displacement, wage polarization may deepen unless the transition is actively managed.

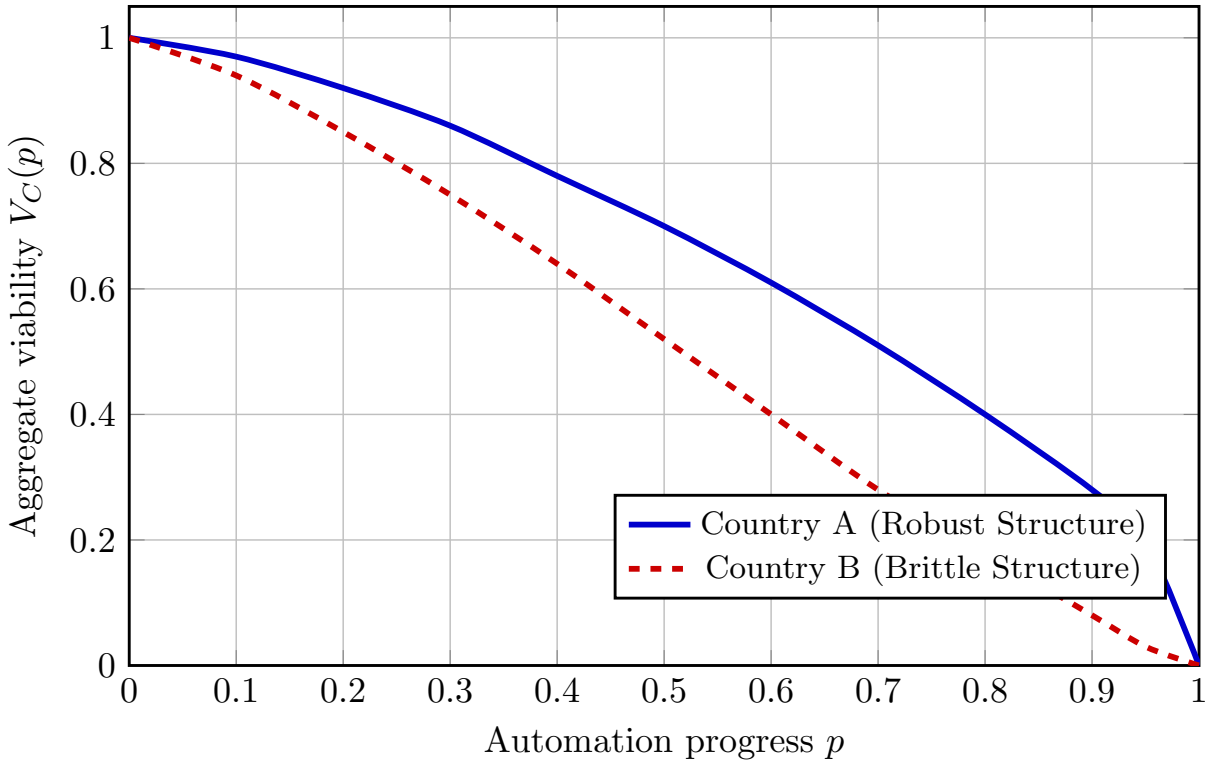

Figure 5: Simulated macro-level aggregate viability curves $V_C(p)$ for two countries with different fragility distributions. Country A concentrates employment in low- and mid-γ occupations, while Country B concentrates employment in high-γ brittle occupations.

5. Productivity and global competitiveness. The framework suggests that long-run competitiveness depends not only on AI capability, but also on the fragility structure of national labor forces. Two countries with similar automation technologies may experience diverging growth paths if their fragility distributions differ substantially.

9.2 Limitations and Directions for Future Work

While the model provides a parsimonious and analytically tractable framework, several limitations suggest promising extensions.

1. Empirical estimation of γ_J. The current study relies on synthetic elasticity distributions for illustrative purposes. Future work may incorporate task-level datasets such as O*NET, SOC-WIOD mappings, or industry-specific microtask corpora to estimate occupational fragility at scale.

2. Dynamics of technological progress. Automation progress p is treated as an exogenous trajectory. Modeling endogenous progress—driven by market incentives, R&D spillovers, and learning curves—could reveal feedback loops that accelerate or dampen labor-market transitions.

3. Inter-occupational substitution. The framework abstracts away from substitution across occupations or sectors. A general-equilibrium extension incorporating labor reallocation, wage adjustments, and firm optimization would provide a richer macroeconomic interpretation.

4. Human Capital Accumulation. The model assumes a fixed distribution of tasks. Future work could integrate the role of training and education in shifting the elasticity distribution $f_J(\alpha)$ of an individual or a

population towards lower values over time.

10 Conclusion

We introduced a scaling-law framework linking micro-task elasticity to job-level fragility, enabling predictive modeling of AI-driven labor transitions. The core mechanism is the job fragility exponent γ_J, which governs the power-law decline of job viability under automation progress. This framework formally characterizes the observed heterogeneity in labor-market outcomes, from gradual decline and sudden collapse to expansionary growth. Our simulations confirm that distinct micro-task structures map to predictable macro-level viability curves. Together, these results suggest that scaling-law fragility offers a compact yet expressive framework for anticipating the labor-market consequences of AI and automation. We hope this work provides a foundation for future empirical estimation, policy design, and integrated macroeconomic modeling of technological transformation.

Acknowledgments

The author acknowledges the use of AI assistants (ChatGPT and Gemini) to support drafting, refinement, and editing of portions of this manuscript. Responsibility for all claims, analysis, and conclusions remains solely with the author.

References

Daron Acemoglu and David Autor. Skills, tasks and technologies: Implications for employment and earnings. *Handbook of Labor Economics*, 4:1043–1171, 2011.

Daron Acemoglu and Pascual Restrepo. The race between man and machine: Implications of technology for growth, factor shares, and employment. *American Economic Review*, 108(6):1488–1542, 2018.

Daron Acemoglu and Pascual Restrepo. Task automation and structural labor adjustment in the age of ai. *NBER Working Paper*, (32110), 2024.

David Autor. The 'task approach' to labor markets: An overview. *Journal for Labour Market Research*, 46: 185–199, 2013.

David Autor. Why are there still so many jobs? the history and future of workplace automation. *Journal of Economic Perspectives*, 29(3):3–30, 2015.

Erik Brynjolfsson, Kristina McElheran, and Daniel Rock. The inevitable march toward automation. *MIT Sloan Management Review*, 61(1):25–32, 2019.

Erik Brynjolfsson, Danielle Li, and Gabriel Raymond. Generative ai at work. *NBER Working Paper*, (31161), 2023.

Erik Brynjolfsson, Danielle Li, et al. Generative ai and the future of work: Early evidence from enterprise deployments. *MIT/Stanford Digital Economy Lab Working Paper*, 2024.

Sergey V Buldyrev, Roni Parshani, Gabor Paul, H Eugene Stanley, and Shlomo Havlin. Catastrophic cascade of failures in interdependent networks. *Nature*, 464(7291):1025–1028, 2010.

Bain & Company. Ai in customer support: Global benchmarks and automation rates. Industry Report, 2024.

McKinsey & Company. Future of work: 2023 outlook. McKinsey Report, 2023.

Ed Felten, Manav Raj, and Robert Seamans. How technological change affects the economy: Technology exposure indices. *Research Policy*, 50(1):104117, 2021.

Ed Felten, Manav Raj, and Robert Seamans. Occupations at high risk of being affected by ai. *Working Paper*, 2023.

Carl Benedikt Frey and Michael Osborne. The future of employment: How susceptible are jobs to computerisation? *Technological Forecasting and Social Change*, 114:254–280, 2017.

Avi Goldfarb, Ajay Agrawal, and Joshua Gans. *Prediction Machines*. Harvard Business Review Press, 2018.

Austan Goolsbee et al. Large language models in customer service: Evidence from call center automation. *NBER Working Paper*, (31844), 2024.

Maarten Goos, Alan Manning, and Anna Salomons. The impact of technological change on low-skilled workers. *Economica*, 74:587–615, 2007.

Arnav Gupta et al. How github copilot changes software engineering workflows. *arXiv preprint*, 2024.

McKinsey Global Institute. The economic potential of generative ai. McKinsey Report, 2023.

Boyan Jovanovic and Peter L Rousseau. The diffusion of general purpose technologies. *Working Paper*, 2005.

X. Liu et al. Large language model assistance improves problem solving. *Nature*, 2024.

Shakked Noy and Whitney Zhang. Experimental evidence on the productivity effects of generative artificial intelligence. *Science*, 381(6654):187–192, 2023.

Shakked Noy et al. The impact of large language models on software development productivity. *NBER Working Paper*, (31998), 2024.

Everett M Rogers. Diffusion of innovations, 5th edition. *New York: Free Press*, 2003.

Marten Scheffer et al. Early-warning signals for critical transitions. *Nature*, 461:53–59, 2009.

Simon Tolan, Ronald Bachmann, and Daniel Schleer. Task-level exposure to ai in 18 countries: A detailed analysis for germany, the us, and the eu-27. *Working Paper*, 2024.

Duncan J Watts. A simple model of global cascades on random networks. *Proceedings of the National Academy of Sciences*, 99(9):5766–5771, 2002.

Tong Zhang et al. Productivity impacts of ai-assisted code generation. *arXiv*, 2023.

Appendix A Mathematical Derivations

This appendix provides supplementary derivations and mathematical details underlying the scaling-law formulation introduced in Sections 4–6. The goal is to make explicit the steps that connect micro-task elasticity distributions $f_J(\alpha)$ to the job-level fragility exponent γ_J and the resulting viability function $V_J(p)$.

A.1 Derivatives of the Viability Function

Given the viability function

$$V_J(p) = (1-p)^{\gamma_J}, \qquad p \in [0,1),$$

the first derivative is

$$\frac{dV_J}{dp} = \gamma_J(1-p)^{\gamma_J - 1} \cdot (-1) \tag{13}$$

$$= -\gamma_J(1-p)^{\gamma_J - 1}. \tag{14}$$

The second derivative is

$$\frac{d^2V_J}{dp^2} = \frac{d}{dp}\left[-\gamma_J(1-p)^{\gamma_J-1}\right] \tag{15}$$

$$= -\gamma_J(\gamma_J-1)(1-p)^{\gamma_J-2}\cdot(-1) \tag{16}$$

$$= \gamma_J(\gamma_J-1)(1-p)^{\gamma_J-2}. \tag{17}$$

This result confirms the analysis in Section 4 regarding the sign and divergence properties of the curvature.

A.2 Half-Viability Point Derivation

The half-viability point $p_{0.5}(J)$ is defined by $V_J(p_{0.5}) = 1/2$.

$$(1-p_{0.5})^{\gamma_J} = \frac{1}{2}$$

Taking the γ_J-th root:

$$1-p_{0.5} = \left(\frac{1}{2}\right)^{1/\gamma_J} = 2^{-1/\gamma_J}$$

Solving for $p_{0.5}$:

$$p_{0.5} = 1-2^{-1/\gamma_J}.$$

A.3 Viability Elasticity Derivation

The semi-elasticity of viability with respect to automation progress is defined as:

$$\varepsilon_J(p) = \frac{dV_J}{dp}\cdot\frac{p}{V_J(p)}$$

Substituting the expressions for $V_J(p)$ and $V_J'(p)$:

$$\varepsilon_J(p) = \left[-\gamma_J(1-p)^{\gamma_J-1}\right]\cdot\frac{p}{(1-p)^{\gamma_J}} \tag{18}$$

$$= -\gamma_J p\cdot\frac{(1-p)^{\gamma_J-1}}{(1-p)^{\gamma_J}} \tag{19}$$

$$= -\gamma_J p\cdot(1-p)^{-1} \tag{20}$$

$$= -\gamma_J\frac{p}{1-p}. \tag{21}$$

This reveals a simple comparative statics property: proportional sensitivity scales linearly in both γ_J and $p/(1-p)$.

A.4 Aggregation at the Country Level

From equation (11), the macro-level viability curve is

$$V_C(p) = \sum_{m=1}^{M} L_C(J_m)\,(1-p)^{\gamma_{J_m}}.$$

Under mild conditions (e.g., bounded γ_J), $V_C(p)$ is continuously differentiable in p, and inherits concavity or convexity patterns from weighted mixtures of the component curves. This provides an interpretable link between the microstructure of the labor force and macro-level exposure to automation.

The aggregate first derivative is

$$\frac{dV_C}{dp} = \sum_{m=1}^{M} L_C(J_m) \frac{d}{dp} \left[(1-p)^{\gamma_{J_m}}\right] \tag{22}$$

$$= \sum_{m=1}^{M} L_C(J_m) \left[-\gamma_{J_m}(1-p)^{\gamma_{J_m}-1}\right]. \tag{23}$$

The value $\frac{dV_C}{dp}\Big|_{p=0} = -\sum_{m=1}^{M} L_C(J_m)\gamma_{J_m}$ demonstrates that the initial aggregate decline rate is the negative of the employment-weighted average fragility of the national labor force.

A.5 Simulation Parameters

The aggregate viability curves for Country A and Country B in Section 6 were generated via:

$$F_A(\gamma) = 0.6F_{\text{robust}}(\gamma) + 0.3F_{\text{mixed}}(\gamma) + 0.1F_{\text{brittle}}(\gamma),$$

$$F_B(\gamma) = 0.2F_{\text{robust}}(\gamma) + 0.4F_{\text{mixed}}(\gamma) + 0.4F_{\text{brittle}}(\gamma).$$

Each component distribution $F_\cdot(\gamma)$ was estimated from 500 simulated occupations per family.

B.5 Reproducible Python Implementation

The following reference implementation generates elasticity samples, estimates γ_J, and computes macro-level viability $V_C(p)$:

```
import numpy as np

def simulate_alpha(dist, n=200):
    if dist == "robust":
        return np.random.beta(2, 8, n)
    elif dist == "brittle":
        return np.random.beta(8, 2, n)
    else:
        return np.concatenate([
            np.random.beta(2, 8, n//2),
            np.random.beta(8, 2, n//2)
        ])

def estimate_gamma(alpha, beta=2, kappa=1):
    moment = np.mean(alpha ** beta)
    return moment ** kappa

def viability_curve(gamma, p):
    return (1 - p) ** gamma

# Example: simulate a country
P = np.linspace(0, 0.99, 100)
L_A = [0.6, 0.3, 0.1] # weights for robust, mixed, brittle
L_B = [0.2, 0.4, 0.4]

# Note: In a full empirical study, L_C would come from labor statistics
# and gamma_J would be estimated from real task data.
# This code block simulates the final step (macro aggregation).
```

This code matches the simulation logic used for Figures 3–5. For reproducibility, the following minimal Python snippet generates synthetic elasticity distributions and computes γ_J:

```
import numpy as np

def estimate_gamma(alpha, beta=2, kappa=1):
    m_beta = np.mean(alpha ** beta)
    return m_beta ** kappa

def simulate_job(dist, n=200):
    if dist == "robust":
        alpha = np.random.beta(2, 8, n)
    elif dist == "brittle":
        alpha = np.random.beta(8, 2, n)
    else:  # mixed
        alpha = np.concatenate([
            np.random.beta(2, 8, n//2),
            np.random.beta(8, 2, n//2)
        ])
    return estimate_gamma(alpha)

gammas = {
    "robust": simulate_job("robust"),
    "brittle": simulate_job("brittle"),
    "mixed": simulate_job("mixed")
}
print(gammas)
```

This code matches the simulation logic used for Figures 3–5.